DOI: 10.1002/ejic.201000758

Synthesis and Characterization of Oligonuclear Ru, Co and Cu Oxidation Catalysts

Bao-Lin Lee,[a] Markus D. Kärkäs,[a] Eric V. Johnston,[a] Andrew K. Inge,[b] Lien-Hoa Tran,[a] Yunhua Xu,[c] Örjan Hansson,[d] Xiaodong Zou,[b] and Björn Åkermark*[a]

Keywords: O-O activation / Homogeneous catalysis / N,O ligands / Oxidation

In this work, we report the preparation and crystal structures of three new oligonuclear complexes, Ru_2(bbpmp)(μ-OAc)$_3$ (**4**), [Co_2(bbpmp)(μ-OAc)(μ-OMe)](PF_6) (**5**), [Cu_4(Hbbpmp)$_2$-(μ-OAc)(H2O)$_2$](OAc)(PF_6)$_2$ (**6**) {H_3bbpmp = 2,6-bis[(2-hydroxybenzyl)-(2-pyridylmethyl)aminomethyl]-4-methylphenol (**3**)}. The structures of the complexes were determined by single-crystal X-ray diffraction. The oxidation states of ruthenium, cobalt and copper in the complexes are +3, +3 and +2, respectively. In **4** and **5**, Ru^{III} and Co^{III} are coordinated to four oxygen and two nitrogen atoms in an octahedral geometry, while in **6**, Cu^{II} adopts both octahedral (CuN_2O_4) and square-pyramidal (CuN_2O_3) geometry. The potential of the three complexes as oxidation catalysts has been investigated.

Introduction

Efficient catalysts for water oxidation are essential for construction of a device that can mimic photosystem II (PSII) in the natural photosynthetic apparatus. The water oxidation catalyst of PSII consists of a tetranuclear manganese cluster, the oxygen evolving complex (OEC).[1] Although a fair number manganese-based OEC mimics have been prepared, none is an efficient water oxidation catalyst.[2] By contrast, several ruthenium complexes, starting with Meyers blue dimer,[3] have been shown to be efficient catalysts.[4]

A dinuclear Mn complex of the anion of ligand **3** (bbpmp) has been studied earlier,[5] but exploratory attempts to use this for catalytic water oxidation have failed. We therefore decided to prepare the related Ru complex **4** and test this. Unfortunately, also complex **4** failed to catalyze water oxidation, probably because of oxidative degradation of the ligand. However, there is a demand for oxidation processes, which use a catalyst and oxygen as terminal oxidant. In these processes oxygen is converted to water, which is the reverse of water oxidation. It therefore seemed interesting to study if **4** and the related cobalt and copper complexes **5** and **6** could be used as catalysts in "green" oxidation of organic substrates by molecular oxygen.

[a] Department of Organic Chemistry, Stockholm University, 10691 Stockholm, Sweden
E-mail: bjorn.akermark@organ.su.se
[b] Structural Chemistry, Department of Materials and Environmental Chemistry, Stockholm University, 10691 Stockholm, Sweden
[c] Department of Chemistry, School of Chemical Science and Engineering, Royal Institute of Technology (KTH), 10044 Stockholm, Sweden
[d] Biophysics Group, Department of Chemistry, University of Gothenburg, P. O. Box 462, 40530 Gothenburg, Sweden
Supporting information for this article is available on the WWW under http://dx.doi.org/10.1002/ejic.201000758.

Results and Discussion

Syntheses and Crystal Structures of 4–6

The ligand **3** was synthesized by using a slightly modified published procedure,[6] (Scheme 1). The bis(chloromethyl) compound **1** was first prepared from 2,6-bis(hydroxymethyl)-4-methylphenol and then reacted with amine **2**, which was in turn prepared by reductive amination of salicylaldehyde with picolylamine.

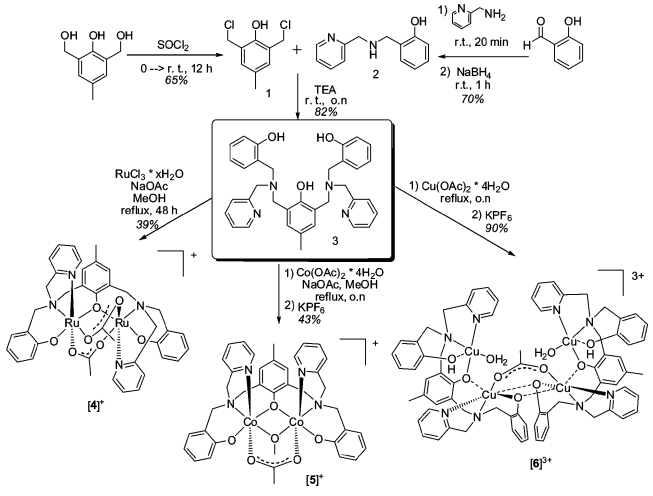

Scheme 1. Syntheses of complexes **4**–**6**.

The ruthenium complex **4** was prepared by adding $RuCl_3 \cdot xH_2O$ and NaOAc to a suspension of ligand **3** in MeOH. The reaction was heated at reflux for 48 h and purified by column chromatography to afford the dark-blue Ru complex.

Complexes **5** and **6** were formed in a similar way by adding NaOAc and $Co(OAc)_2 \cdot 4H_2O$ or $Cu(OAc)_2 \cdot 4H_2O$, respectively, to a suspension of ligand **3** in MeOH. The reaction mixture was heated at reflux overnight, then cooled and filtered, and finally KPF_6 was added. The copper complex **6** precipitated directly and could be isolated as a green powder, while the cobalt complex **5** required a couple of days to precipitate as a brown solid.

The crystal structures of the metal complexes **4**, **5** and **6** were determined from single-crystal X-ray diffraction data. The crystal data and structure refinement parameters are given in Table 3. Selected bond lengths of **4**, **5**, and **6** are listed in Table S1.

The crystal structure of **4** contains one unique $[Ru_2(bbpmp)(\mu\text{-}OAc)_2]^+$ complex and seven unique water molecules. The two ruthenium atoms have similar octahedral coordination environments, each coordinated to one pyridyl and one tertiary amine nitrogen atom, two phenolate oxygen atoms, and two oxygen atoms from two different acetates. The ruthenium atoms are bridged by one oxygen atom of the central phenolate of the bbpmp and two bidentate acetates (Figure 1). The dinuclear Ru complex adopts a pseudo-twofold symmetry through the C–O bond of the bridging phenolate, which is similar to that in $[Fe_2(bbpmp)(\mu\text{-}OAc_2)]ClO_4 \cdot H_2O$.[7] The bond valence sum (BVS) for each ruthenium centre is 3.25, which suggests that the oxidation state of both ruthenium atoms is 3. This is also supported by mass spectrometry (MS), UV/Vis and EPR spectroscopy, and cyclic voltammetry (CV). Seven unique oxygen positions, which form hydrogen bonds to the two terminal phenolate oxygen atoms and one acetate oxygen atom, were located in the structure refinement. However, the third acetate counterion, which is suggested by elemental analysis, could not be located, presumably because of disorder in the crystal. The actetate counterion is strongly suggested by the fact that the complex has a $Ru_2^{III/III}$ oxidation state.

There seem to be few X-ray crystal structures known for complexes related to **4**, but it is interesting to compare the Ru-phenolate bond length of **4** to those of other phenolate complexes of ruthenium of different oxidation states. The Ru–O bond to the terminal phenolate is ca 1.95 Å in **4**, which seems to be unusually short. In two formally Ru^{III} diamide-phenolate complexes, the Ru–O bond is distinctly longer, ca. 2.03 Å.[8] Even longer Ru–O phenolate distances were observed for a series of mononuclear Ru^{II} complexes with a bidentate N–O(phenolate) ligand (2.03–2.10 Å),[9–11] and in a formally Ru^{III} biscarbene complex, the bond length is 2.27 Å.[12] The significance of the short Ru–O bond in **4** is not clear, but perhaps it is the result of an unusually electrophilic Ru^{III} centre. The ligand in the complex should be fairly rigid, as indicated by the structure of the complex **4** (Figure 1). This could lead to steric effects in the coordination of the alcohols, which could explain the relatively inefficient oxidation of secondary alcohols to ketones.

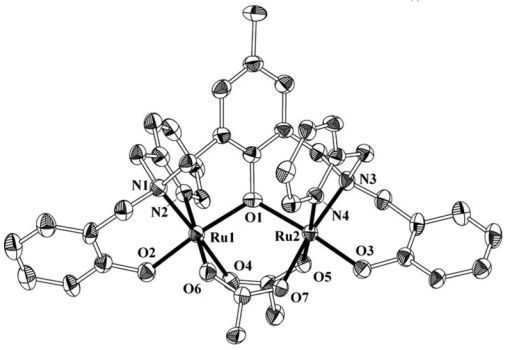

Figure 1. X-ray structure of the cation $[Ru_2(bbpmp)(\mu\text{-}OAc)_2]^+$ from **4** at a 30% probability level. Hydrogen atoms and solvent molecules are omitted for clarity.

The crystal structure of **5** contains one unique $[Co_2(bbpmp)(\mu\text{-}OAc)(\mu\text{-}OMe)]^+$ complex and one unique hexafluorophosphate anion. As in complex **4**, the two cobalt atoms are octahedrally coordinated (Figure 2), each to two nitrogen atoms and two oxygen atoms of the bbpmp ligand, one oxygen atom of the bridging acetate, and the oxygen atom of the bridging methoxy group. The dinuclear Co^{III} complex adopts a pseudomirror symmetry with the mirror plane perpendicular to Co(1)–O–Co(2). BVS calculations indicate that all oxygen atoms of the ligands are deprotonated, which suggests that both cobalt atoms have a charge of +3. This is in accord with an earlier report, which shows that cobalt complexes prepared from Co^{II} and phenolic ligands are readily converted to Co^{III} complexes.[13]

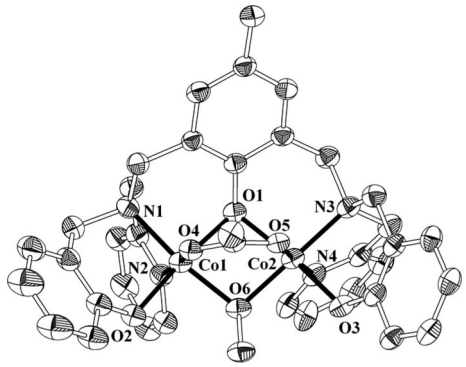

Figure 2. X-ray structure of the cation $[Co_2(bbpmp)(\mu\text{-}OAc)(\mu\text{-}OMe)]^+$ from **5** at a 30% probability level. Hydrogen atoms and solvent molecules are omitted for clarity.

Somewhat surprisingly, the copper complex **6** crystallizes as a linear tetramer. The crystal structure contains one unique $[Cu_4(Hbbpmp)_2(\mu\text{-}OAc)(H_2O)_2]^{3+}$ complex. The +3 charge is balanced by two unique hexafluorophosphate anions and one unique hydrogen-bonded acetate group. The two central copper atoms of the tetranuclear complex adopt a distorted octahedral coordination, while the two terminal copper atoms adopt a square-pyramidal coordination (Fig-

ure 3). As in the metal centres in **4** and **5**, each copper ion is coordinated to one pyridyl and one tertiary amine nitrogen atom. In addition, each central copper atom is coordinated to three phenolate groups and one acetate oxygen atom, while each terminal copper atom is coordinated to one phenolate, one phenol and one water oxygen atom. The central copper atoms are bridged through one acetate and two phenolate groups from two different bbpmp ligands, while the terminal and central copper atoms are bridged through one phenolate only.

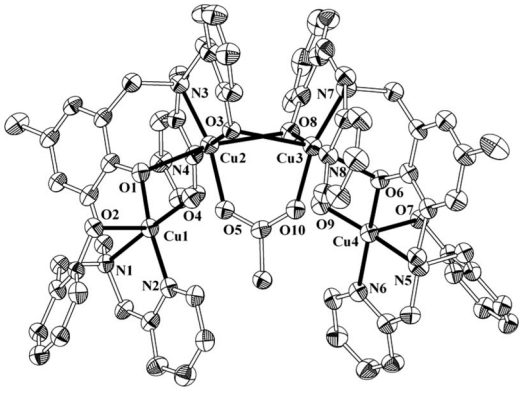

Figure 3. X-ray structure of the trication $[Cu_4(Hbbpmp)_2(\mu\text{-}OAc)(H_2O)_2]^{3+}$ from **6** at a 30% probability level. Hydrogen atoms and solvent molecules are omitted for clarity.

The tetranuclear copper complex adopts a pseudo-twofold symmetry along the C–C bond of the bridging acetate between the central copper atoms Cu2 and Cu3. The distorted coordination at the axial positions is a result of the Jahn–Teller effect, common for Cu^{II} complexes. The terminal copper atoms, Cu1 and Cu4, have identical coordination environments, in which amine and pyridyl nitrogen atoms of the bbpmp ligand are coordinated *cis* relative to one another, and one oxygen atom of a central phenolate group and one water molecule complete coordination in the equatorial plane. The terminal phenol groups in the axial position have considerably longer bonds to the Cu^{II} atoms (2.41 and 2.44 Å) than the bridging phenolate groups (1.89 and 1.91 Å). The low bond valence with an average value of 0.135 between Cu and the terminal phenol oxygen atoms O2 and O7 and the long bonds suggest that these phenol groups are protonated. Similarly, the phenol groups coordinated axially to Cu^{II} in the alkoxide-bridged complex $[Cu_2(H_2bbppnol)(OAc)(H_2O)_2]Cl_2{\cdot}2H_2O$ have been reported to have protonated oxygen atoms.[14]

A comparison of the three complexes shows that the Ru–Ru atoms in **4**, the Co–Co atoms in **5** and the central Cu–Cu atoms in **6** are bridged by three molecules: one phenolate and two acetate groups in **4**, one phenolate, one acetate and one methoxy group in **5**, and two phenolate groups and one acetate group in **6**. By contrast, the terminal and central copper atoms in **6** are bridged through only one phenolate group. This together with the fact that the terminal copper atoms are only five-coordinate suggest that the complex should rearrange and dissociate to dinuclear complexes fairly readily. The fact that the cobalt atoms in **5** and the central copper atoms in **6** have two M–O–M connections results in much smaller M–O–M (93.7°–99.2°) and O–M–O (80.5°–82.0°) angles than the corresponding angles when there is only one M–O–M connection: 110.0°–119.6° and ca. 90°, as in **4** and between the terminal and central copper atoms in **6**, respectively (see Table S1).

The Co–Co distance (2.90 Å) in **5** is much smaller than the Ru–Ru distance (3.50 Å) in **4**, partly because of the double Co–O–Co bridges. However, the central copper atoms also have double bridges, yet the Cu–Cu distance is fairly long (3.28 Å). This is due to the longer distances from copper to the axial oxygen atoms, caused by the Jahn–Teller effect. This effect is shown even more clearly by the long Cu–Cu distance between the terminal and central copper atoms (3.49–3.70 Å).

The octahedra in **5** are more distorted than those in **4**, because of the double M–O–M bridges and the octahedra in **6** are even more so because of both the double Cu–O–Cu bridges (Cu central) and the Jahn–Teller effect. In all complexes, the amine and pyridyl groups from the same bbpmp ligand are coordinated in a *cis* fashion to the metal ions, with an N–M–N angle between 81.8° and 84.4°, which indicates a geometrical strain in the ligand. The phenolate groups from the same bbpmp ligand are coordinated in a *trans* manner to the metal ions in **4** and **5**, but *cis* to the metal ions in **6**.

The complexes **4** and **6** have pseudo-twofold symmetry, while **5** has a pseudomirror symmetry. In **4** and **6**, there are π–π interactions between the phenolate and pyridyl rings, but not in **5** because of the short Co–Co distance. Additionally, in complex **6**, the terminal phenol and pyridyl rings, which are coordinated to the same terminal copper atom, can also interact as a result of the longer axial coordination to the phenol oxygen atom. Finally, both bridging acetate groups in **4** are coordinated in a *trans* fashion to the amine and pyridine groups, while in **5**, the acetate is coordinated in a *trans* manner only to the pyridine groups, and in **6**, only to the amine groups.

Electrochemistry

The cyclic voltammograms of ligand **3** and complexes **4**–**6** were recorded in 1 mM solution in acetonitrile (MeCN) with Bu_4NPF_6 as the supporting electrolyte, a glassy carbon disk as the working electrode and $Ag/AgNO_3$ as the reference electrode in the potential range of –2.0 to +2.0 V vs. Ag/Ag^+. The potentials were measured vs. Fc^+/Fc^0 and converted to potentials vs. NHE by adding +0.63 V. The cyclic voltammograms of **3** and complexes **4** and **5** are shown in Figure 4. The copper complex **6** did not give a proper CV but there are indications of redox peaks at –1.17 and –0.81 V vs. NHE that can perhaps be ascribed to $Cu^{II}Cu^{II} \rightarrow Cu^{II}Cu^{I}$ and $Cu^{II}Cu^{I} \rightarrow Cu^{I}Cu^{I}$ processes in accordance with a previous report on a related alkoxide-bridged complex.[15]

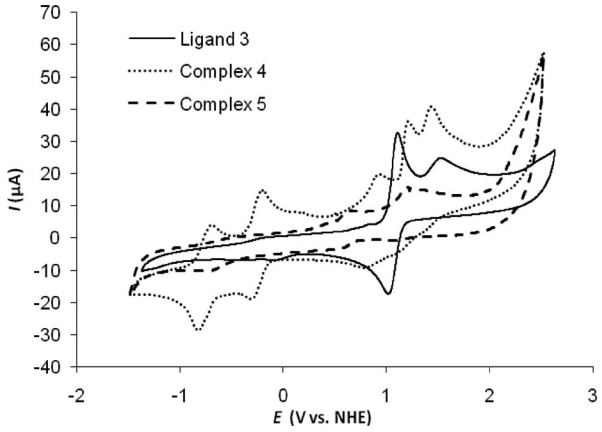

Figure 4. Cyclic voltammograms of ligand **3** and complexes **4** and **5**. Conditions: 1.0 mM of **3**, **4** or **5** in MeCN with 0.1 M Bu_4NPF_6 as supporting electrolyte.

The electrochemistry of the Ru complex **4** exhibits two reversible one-electron redox couples with $E_{1/2}$ values of –0.76 and –0.25 V vs. NHE, which are assigned to the reductions $Ru^{III}Ru^{II} \rightarrow Ru^{II}Ru^{II}$ and $Ru^{III}Ru^{III} \rightarrow Ru^{III}Ru^{II}$, respectively, and a irreversible peak at E_{pa} = +0.94 V vs. NHE, which is assigned to the oxidation $Ru^{III}Ru^{III} \rightarrow Ru^{IV}$-$Ru^{III}$. This may be compared with the values of $Ru^{III}Ru^{II} \rightarrow Ru^{II}Ru^{II}$ and $Ru^{III}Ru^{III} \rightarrow Ru^{III}Ru^{II}$ for the related dinuclear Ru complex containing the monoanionic ligand 2,6-bis[bis(2-pyridylmethyl)aminomethyl]-4-methylphenol, with $E_{1/2}$ values of +0.02 and +0.72 V vs. NHE.[16] These metal-centred oxidations for complex **4** are thus lowered by 0.78 and 0.97 V, respectively, which is close to the values observed earlier for tris(bipyridine)-type complexes, where the oxidation potential decreases by ca 0.4 V per added negative substituent, in this case, the carboxylate groups.[17] Two irreversible oxidation peaks are also observed at ca. 1.24 and 1.46 V vs. NHE, tentatively assigned to ligand oxidations. The values for **4** are also close to those found for a similar complex, where the terminal phenol groups of the ligand are di-*tert*-butylphenol instead of a simple phenol (–0.85, –0.62 and +0.75 V vs. NHE).[18] The Co complex **5** shows one reversible redox couple with an $E_{1/2}$ value of +0.72 V vs. NHE, one quasireversible reduction peak at –0.70 V vs. NHE and one irreversible oxidation peak at +1.25 V vs. NHE.

UV/Vis Spectroscopy

The UV/Vis spectra of ligand **3** and complexes **4**–**6** were recorded in acetonitrile and are shown in Figure 5. The spectra of the Co and Cu complexes **5** and **6**, respectively, are quite similar, and lack intense absorption bands in the region above 550 nm. The Co complex **5** has a broad absorption band at 406 nm (ε = 3128 $M^{-1}cm^{-1}$) with a shoulder at 480 nm (ε = 2470 $M^{-1}cm^{-1}$). The spectrum of the Cu complex **6** shows a broad absorption band at 438 nm (ε = 2840 $M^{-1}cm^{-1}$) and a shoulder at 470 nm (ε = 2230 $M^{-1}cm^{-1}$).

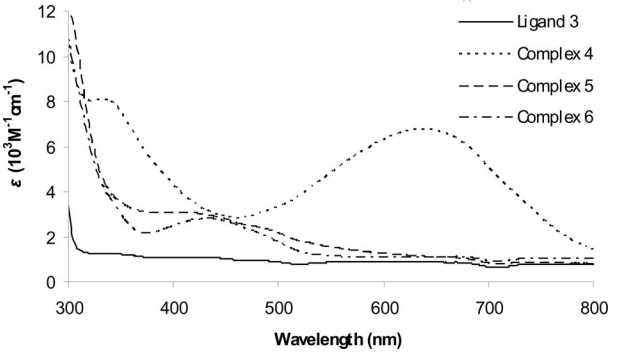

Figure 5. UV/Vis absorption spectra of ligand **3** and complexes **4**–**6** in dry acetonitrile (c = 0.1 mM).

By contrast, the Ru complex **4** displays a strong and broad visible absorption with a peak at 634 nm (ε = 6820 $M^{-1}cm^{-1}$), which can be assigned to a LMCT transition, and a band at 331 nm (ε = 8150 $M^{-1}cm^{-1}$). This spectrum closely resembles that of the dinuclear $Ru^{III/III}$ complex containing the ligand 2,6-bis[bis(2-pyridylmethyl)-aminomethyl]-4-methylphenol and supports the predicted oxidation state of complex **4**.[16,18]

EPR Spectroscopy

The Ru complex **4** was also studied with X-band EPR spectroscopy at 77 K. Frozen solutions of **4** at a concentration of 1 mM in either dcm, chloroform or thf gave only weak signals with g values of approximately 2.39, 2.28, and 1.72. These are probably due to the small amount of mixed valence species ($Ru_2^{II/III}$ or $Ru_2^{III/IV}$),[16] while the major part of the complexes resides in the EPR-silent $Ru_2^{III/III}$ state.

Catalytic Activity

The oxidation of alcohols to ketones and aldehydes with ruthenium catalysts has been studied extensively earlier.[19a] Both $RuCl_3$ and $RuCl_2(Ph_3P)_2$,[19b] and trinuclear ruthenium carboxylates[19c] have been shown to be viable catalysts for the aerobic oxidation of alcohols to aldehydes and ketones.

In order to study the catalytic properties of complex **4**, we first tried the oxidation of benzylic alcohols by using oxygen as the oxidant. The results proved to be difficult to reproduce, which suggested that the aromatic nucleus was oxidized. Hydrogen peroxide and *tert*-butyl hydroperoxide were also evaluated as oxidants, and benzyl alcohol was the model substrate. Although they gave good conversion, the selectivity was poor (aldehyde/carboxylic acid 1:1). However, with diacetoxyiodobenzene as oxidant, which should give a Ru-oxo intermediate, the aldehyde was obtained in excellent yield and selectivity (Scheme 2, Table 1).

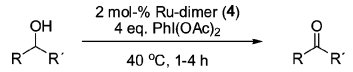

Scheme 2. Oxidation of alcohols with Ru complex **4** as catalyst.

Table 1. Oxidation of alcohols with Ru complex **4** as catalyst.[a]

Entry	Substrate	Product	Time (h)	Conversion[b] (%)	Yield[b] (%)
1			1	>99	99[c]
2			4	>99	90
3			4	53	53[d]
4	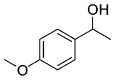	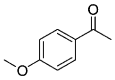	4	54	54
5			1	>99	91
6	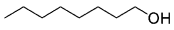	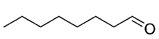	1	>99	98[c,e]
7	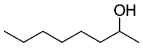	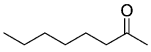	4	34	32

[a] Complex **4** (0.003 mmol) and dodecane (0.15 mmol) were dissolved in dry MeCN/THF (1 mL, 1:1). The substrate (0.15 mmol) and iodobenzene diacetate (0.6 mmol) were added. The mixture was degassed and flushed with argon and heated to 40 °C. [b] Determined by GC, with dodecane as internal standard {yield (%) = $[n_{prod.}]/[n_{subs.(t=0)}]\times100$; conversion (%) = $(1 - [n_{subs.}]/[n_{subs.(t=0)}])\times100$}. [c] <1% of the corresponding carboxylic acid was observed. [d] 73% after 20 h. [e] Decane was used as internal standard.

Both benzylic and aliphatic primary alcohols could be converted into the corresponding aldehydes in excellent yield and selectivity (only traces of the carboxylic acid were observed). The oxidation of secondary alcohols was less efficient (see Table 1, Entries 3, 4 and 7), with the exception of the cyclic alcohol, indanol (Entry 2). The result could perhaps be due to steric hindrance, caused by the fairly tight structure of complex **4**.

Control experiments, without catalyst **4**, were performed and resulted in ca. 10% conversion.

The introduction of electron-donating groups, expected to give more electron-rich substrates, was expected to facilitate the oxidation of alcohol to ketone. However, no such effect could be observed (Entries 3 and 4). The introduction of a methyl group at the *ortho* position on the aromatic ring was expected to cause steric hindrance and slow down the reaction. 2-Methylbenzyl alcohol was chosen as the substrate, but the reaction gave essentially the same high yield as the parent benzyl alcohol (see Table 1, Entries 1 and 5).

It has been demonstrated earlier that Co and Cu complexes are effective catalysts for the activation of molecular oxygen.[20] We therefore decided to evaluate the potential of our newly synthesized catalysts in coupled aerobic oxidation reactions (Scheme 3).

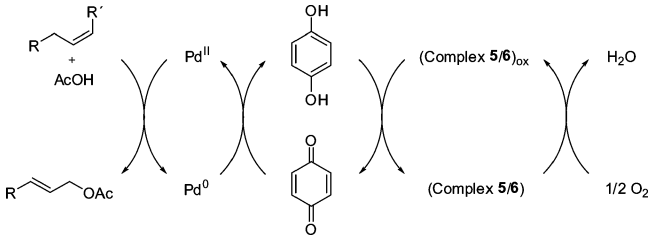

Scheme 3. Coupled aerobic oxidation, where complexes **5** and **6** were evaluated as oxygen-activating catalysts.

The cobalt complex **5** was tested as an oxygen-activating catalyst in allylic acetoxylation of alkenes (Scheme 4).[21,22] Three different olefins were studied, cyclohexene, allylbenzene and 1-octene. The corresponding allylic acetates were formed in moderate yields (Table 2). However, the reaction was not optimized since it was only used for demonstrating the properties of complex **5**, and complete conversion of the alkenes was in fact observed. Complex **5** thus appears to compare favourably with common oxygen-activating catalysts, such as cobalt salen complexes[22] and phthalocyanins.[21b,23].

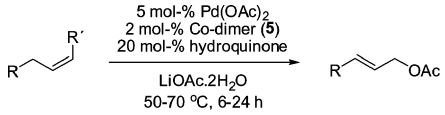

Scheme 4. Aerobic acetoxylation, where Co complex **5** was used as an oxygen-activating catalyst.

Table 2. Biomimetic aerobic acetoxylation of olefins with Co complex **5** as oxygen-activating catalyst.[a]

Entry	Substrate	Product	Time (h)	Yield[b] (%)
1			6	63
2	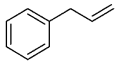	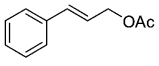	24	54
3	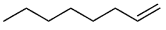	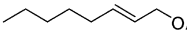	14	58

[a] $Pd(OAc)_2$ (0.034 mmol), hydroquinone (0.14 mmol), $LiOAc{\cdot}2H_2O$ (0.14 mmol) and complex **5** (0.014 mmol) were dissolved in AcOH (2 mL). The mixture was stirred under air for 20 min, and the flask was then sealed, degassed and purged with oxygen. Finally, the substrate (0.68 mmol) was added, and the reaction mixture was heated to 50 °C. [b] Isolated yield.

The Cu complex **6** shows no activity as an oxygen-activating catalyst in the aerobic acetoxylation of olefins, presumably because the oxidation of palladium(0) is too slow to compete with precipitation of metallic palladium. However, like the related dinuclear Cu complex with a bridging alkoxide group,[15] it did function as a catalyst for the aerobic oxidation of 3,5-di-*tert*-butylcatechol. It is thus a catecholase mimic, and the rate of oxidation is comparable to that of the alkoxide-bridged complex.[15]

Conclusions

The ruthenium, cobalt and copper complexes are efficient catalysts for different reactions such as the oxidation of alcohols to aldehydes and ketones, allylic oxidation and the oxidation of 3,5-di-*tert*-butylcatechol to the corresponding *ortho*-quinone. This suggests that the configuration of ligand **3**, in which there are three phenolate groups and two amine functions that can bind at least two metal ions, is a favourable arrangement for producing efficient oxidation catalysts. Although all complexes efficiently activate oxygen, there are substantial differences in their catalytic activity. Since the oxidation of alcohols probably proceeds through β-elimination, one can perhaps conclude that more facile β-elimination with ruthenium is the reason that this catalyst is more efficient than the others. None of the complexes is capable of catalyzing water oxidation, probably because the ligand is oxidized at the required high oxidation potentials. However, the copper complex **6** is very interesting in relation to water oxidation, since it is tetranuclear, as is the manganese complex in the OEC of PSII.[1] Because the oxidation of catechol is not cleanly first order, it is probable that **6** is partly dissociated in solution. However, it is interesting to compare it with the dinuclear alkoxide-bridged complex, which reacts with catechol in a second order reaction.[15] This suggestsg that the reactive intermediate is in fact tetranuclear. This ease of formation of a tetranuclear complex suggests that also other metals, e.g. manganese, might form tetranuclear complexes as intermediates with ligands related to compound **3**. On the basis of these results with complexes of ligand **3**, we are now focusing on the synthesis of such ligands, which are more stable towards oxidative degradation.

Experimental Section

Chemicals were purchased from commercial suppliers at reagent grade purity or better and used without further purification unless otherwise stated. All solvents were dried by standard methods when needed. ^{1}H NMR and ^{13}C NMR were recorded on a 400 MHz spectrometer using [D$_1$]chloroform (δ =7.26 ppm ^{1}H, 77 ppm ^{13}C) as internal standard. Flash chromatography was carried out with a 60-Å (particle size 35–70 μm) normal-phase silica gel. High resolution mass spectra measurements were recorded on a Bruker Daltonics microTOF spectrometer with an electrospray ionizer. Cyclic voltammetry measurements were carried out with an Autolab potentiostat with a GPES electrochemical interface (Eco Chemie), by using a glassy carbon disk (diameter 3 mm) as the working electrode, a platinum wire as counter electrode. The reference electrode was a non-aqueous Ag/Ag$^+$ electrode (0.1 M $AgNO_3$ in acetonitrile). The supporting electrolyte used was 0.1 M Bu_4NPF_6 in acetonitrile. The reference electrode had a potential of –0.055 vs. the ferrocenium/ferrocene ($Fc^{+/0}$) couple in acetonitrile as an external standard. All potentials reported were determined vs. $Fc^{+/0}$. They are reported vs. NHE by adding 0.63 V to the $E_{1/2}$ value of $Fc^{+/0}$. Half-wave potentials ($E_{1/2}$) were determined by CV as the average of the anodic and cathodic peak potentials [$E_{1/2}$ = (E_{pa} + E_{pc})/2]. Reversibility was confirmed by peak splits of ΔE = 60–70 mV and i_{pa}/i_{pc} = 1. IR spectra were recorded on a Perkin–Elmer Spectrum One spectrometer by using samples prepared as KBr discs. The UV/Vis absorption spectra were measured on a CARY 300 Bio UV/Vis spectrophotometer.

EPR spectra were recorded at 77 K on a Varian E9 spectrometer equipped with a quartz insert for liquid nitrogen. Measurements were made with a microwave frequency of 9.12 GHz, a microwave power of 2 mW and a modulation amplitude of 2 mT.

Single crystal X-ray diffraction data of **4** (dark-blue platelike crystal), **5** (brown plate crystal) and **6** (green platelike crystal) were collected on a MarCCD at 100 K by using synchrotron radiation (λ = 0.9077 Å) at the beam line I-911–2, Max Lab, Sweden. Twinsolve was used for indexing, data reduction, and numerical absorption correction on the data. The structures were solved by direct methods with SHELXS97.[24] All non-hydrogen atoms of the complexes were refined with anisotropic thermal parameters by using a full-matrix least-squares technique on F^2 with SHELXL97.[24] Hydrogen atoms were geometrically positioned. The thermal displacement parameters of hydrogen atoms were set to 1.2 times the thermal parameter of the bonded aromatic carbon or 1.5 times the thermal parameter of the bonded methyl carbon. Intensity data was truncated at a resolution of 0.86 Å for **6**. One of the toluene molecules in **6** was disordered into two positions with an occupancy of 0.5 each. Crystallographic details of **4**, **5** and **6** are provided in Table 3. SQUEEZE was applied by using PLATON to manage solvent accessible voids.[25] BVS values were obtained from Bond Valence Calculator.[26] CCDC-783630 (for **4**), -783631 (for **5**) and -783632 (for **6**) contain the supplementary crystallographic data for this paper. These data can be obtained free of charge from The Cambridge Crystallographic Data Centre via www.ccdc.cam.ac.uk/data_request/cif.

Synthesis of 2,6-Bis(chloromethyl)-4-methylphenol (1): 2,6-Bis-(hydroxymethy1)-4-methylphenol (2.50 g, 14.9 mmol) was added to $SOCl_2$ (20 mL) at 0 °C. After warming to ambient temperature, the reaction was stirred for 12 h and $SOCl_2$ was evaporated. The remaining residue was dissolved in CH_2Cl_2 and washed with water (3 × 50 mL) and dried with anhydrous $MgSO_4$. The dried solution was partly evaporated at reduced pressure. Pentane was layered on top, and the flask was put in the refrigerator to give crystals, which were filtered and washed with pentane to give the title compound as yellow–grey needles (1.98 g, 65%). ^{1}H NMR (400 MHz, $CDCl_3$, 25 °C): δ = 7.09 (s, 2 H, Ar-H), 4.66 (s, 4 H, 2 CH_2), 2.28 (s, 3 H, CH_3) ppm. ^{13}C NMR (100 MHz, $CDCl_3$, 25 °C): δ = 150.99, 131.61, 130.55, 124.63, 42.48, 20.32 ppm. ESI-HRMS calcd. for $C_9H_{10}Cl_3O$ [M + Cl$^-$] 238.9803; found 238.9809.

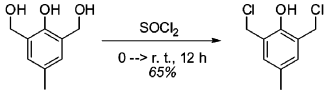

Synthesis of (2-Hydroxybenzyl)(2-pyridylmethyl)amine (2): To a solution of salicylaldehyde (0.61 g, 5.0 mmol) in MeOH (10 mL) was added 2-(aminomethyl)pyridine (0.54 g, 5.0 mmol). The clear yellow solution was stirred at ambient temperature for 20 min. At ambient temperature, $NaBH_4$ (0.19 g, 5.00 mmol) was added in small portions, which led to the development of a gas. The reaction mixture became colourless. After stirring at ambient temperature for 1 h, the solvent was evaporated. H_2O (10 mL) was added to the residue, and the pH was adjusted to 7 by 2 M HCl. The solution was extracted with CH_2Cl_2 (3 × 6 mL). The organic phases were combined and dried with $MgSO_4$. Evaporation of the solvent gave light-brown crystals. Purification by silica flash chromatography (EtOAc) gave the desired product as pale-yellow crystals (0.76 g, 70%). ^{1}H NMR (400 MHz, $CDCl_3$, 25 °C): δ = 8.56–8.59 (m, 1 H,

Table 3. Crystal data and structure refinement for complexes **4**, **5** and **6**.

	4·7H_2O	**5**	**6**·2(toluene)
Empirical formula	$C_{41}H_{56}N_4O_{16}Ru_2$[a]	$C_{38}H_{39}Co_2F_6N_4O_6P$	$C_{88}H_{94}Cu_4F_{12}N_8O_{12}P_2$
F_w	1063.04 [a]	910.56	1999.81
T (K)	100	100	100
Wavelength (Å)	0.9077	0.9077	0.9077
Crystal system	orthorhombic	monoclinic	monoclinic
Space group	*Pbca*	*C*2/*c*	$P2_1/n$
a (Å)	13.476(3)	30.779(6)	14.922(3)
b (Å)	20.816(4)	18.618(4)	25.504(5)
c (Å)	30.892(6)	15.661(3)	24.265(5)
β (°)	–	109.61(3)	103.87(3)
V (Å^3)	8665(3)	8454(3)	8965(3)
Z	8	8	4
$D_{calcd.}$ (g/cm^3)	1.517	1.431	1.482
Absorption coefficient (mm^{-1})	0.765	0.897	1.061
F(000)	4008	3728	4112
Crystal size (mm)	0.021 × 0.086 × 0.097	0.028 × 0.071 × 0.117	0.042 × 0.080 × 0.226
θ range for data collection (°)	3.27 to 32.27	3.53 to 33.45	3.25 to 31.85
Index ranges	$-15 \le h \le 15$, $-24 \le k \le 24$, $-36 \le l \le 36$	$-37 \le h \le 37$, $-20 \le k \le 20$, $-18 \le l \le 18$	$-17 \le h \le 17$, $-29 \le k \le 29$, $-27 \le l \le 27$
Reflections collected	102439	53836	103476
Independent reflections	7771 [R(int) = 0.1130]	7422 [R(int) = 0.0572]	13866 [R(int) = 0.0779]
Completeness to θ_{max} (%)	0.997 to θ = 32.27°	0.935 to θ = 33.45°	0.939 to θ = 31.85°
Absorption correction	empirical	empirical	empirical
Max. and min. transmission	1.000 and 0.9823	1.000 and 0.9734	1.000 and 0.9829
Refinement method	full-matrix least squares on F^2	full-matrix least squares on F^2	full-matrix least squares on F^2
Data/restraints/parameters	7365/0/369	7422/0/390	13866/5/721
Goodness-of-fit on F^2	1.001	1.051	1.058
Final R indices [$I > 2\sigma(I)$]	$R1$ = 0.0940, $wR2$ = 0.2537	$R1$ = 0.0670, $wR2$ = 0.1869	$R1$ = 0.0905, $wR2$ = 0.2424
R indices (all data)	$R1$ = 0.1174, $wR2$ = 0.2704	$R1$ = 0.0839, $wR2$ = 0.1978	$R1$ = 0.1159, $wR2$ = 0.2615
Largest diff. peak and hole (e/Å^3)	1.699 and –0.916	0.539 and –0.586	1.011 and –1.275

[a] Empirical formula includes acetate and hydrogen atoms of crystalline water molecules that were excluded in the structure refinement.

pyr-H), 7.65 (td, J = 7.61, 1.73 Hz, 1 H, pyr-H), 7.18–7.22 (m, 2 H, pyr-H), 7.16 (m, 1 H, Ar-H), 6.96 (m, 1 H, Ar-H), 6.86 (dd, J = 8.08, 1.18 Hz, 1 H, Ar-H), 6.78 (td, J = 7.40, 1.30 Hz, 1 H, Ar-H), 4.00 (s, 2 H, CH_2), 3.91 (s, 2 H, CH_2) ppm. ^{13}C NMR (100 MHz, $CDCl_3$, 25 °C): δ = 158.24, 157.79, 149.47, 136.68, 128.79, 128.60, 122.69, 122.42, 119.03, 116.44, 53.09, 51.91 ppm. ESI-HRMS calcd. for $C_{13}H_{15}N_2O$ [M + H$^+$] 215.1179; found 215.1189.

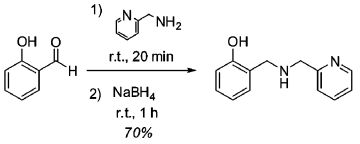

Synthesis of 2,6-Bis[(2-hydroxybenzyl)(2-pyridylmethyl)aminomethyl]-4-methylphenol (3): (2-Hydroxybenzyl)(2-pyridylmethyl)amine (5.22 g, 24.4 mmol) was added to a solution of 2,6-bis(chloromethyl)-4-methylphenol (2.50 g, 12.2 mmol) in CH_2Cl_2 (40 mL). The reaction mixture turned brown and cloudy. When Et_3N (8.5 mL, 61 mmol) was added, the reaction mixture turned light brown, and a precipitate formed. After stirring at ambient temperature overnight, the reaction mixture was diluted with CH_2Cl_2 (20 mL), washed with brine (4 × 50 mL), dried with $MgSO_4$ and evaporated to give a brown oil. Recrystallization from CH_2Cl_2/2-propanol gave a white solid, which was filtered and washed with 2-propanol to give **3** (5.58 g, 82%). ^{1}H NMR (400 MHz, $CDCl_3$, 25 °C): δ = 8.60–8.64 (d, J = 4.74 Hz, 2 H, pyr-H), 7.62–7.69 (td, J = 7.97, 1.74 Hz, 2 H, pyr-H), 7.11–7.25 (m, 4 H, pyr-H), 7.11–7.17 (t, J = 7.97 Hz, 2 H, Ar-H), 7.00–7.05 (d, J = 7.73 Hz, 2 H, Ar-H), 6.88 (s, 2 H, Ar-H), 6.79–6.85 (d, J = 7.97 Hz, 2 H, Ar-H), 6.73–6.78 (t, J = 7.73 Hz, 2 H, Ar-H), 3.85 (s, 4 H, 2 CH_2), 3.81 (s, 4 H, 2 CH_2), 3.77 (s, 4 H, 2 CH_2), 2.21 (s, 3 H, CH_3) ppm. ^{13}C NMR (100 MHz, $CDCl_3$, 25 °C): δ = 157.55, 157.22, 153.75, 148.47, 137.00, 131.11, 129.90, 128.93, 127.74, 123.55, 122.80, 122.31, 118.96, 116.52, 57.57, 56.68, 54.55, 20.45 ppm. IR (KBr disc): $\tilde{\nu}$ = 3600–2400 (br.), 3406, 3041, 3010, 2913, 2835, 2814, 2700, 1600, 1592, 1488, 1430, 1368, 1304, 1265, 1253, 1228, 1096, 968, 865, 757 cm^{-1}. ESI-HRMS calcd. for $C_{35}H_{37}N_4O_3$ [M + H$^+$] 561.2860; found 561.2879.

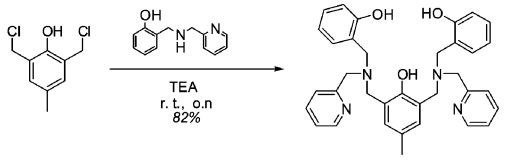

Synthesis of Ru_2(bbpmp)$(OAc)_3$ (4): $RuCl_3 \cdot xH_2O$ (0.50 g, 1.9 mmol) and NaOAc (0.88 g, 10.7 mmol) was added to a suspension of ligand **3** (0.50 g, 0.89 mmol) in MeOH (25 mL). The dark solution was heated at reflux for 48 h and then cooled to room temperature. After the solvent was evaporated, acetone was added, and the insoluble salts were filtered. Evaporation of the filtrate gave a dark solid, which was purified by silica flash chromatography (MeCN/H_2O/NEt_3, 90:10:5) to give **4** as a dark-blue solid (0.31 g, 39%). IR (KBr disc): $\tilde{\nu}$ = 3400(br.), 2913, 2844, 1609, 1555, 1477, 1447, 1412, 1381, 1262, 1153, 1108, 1031, 883, 761 cm^{-1}. ESI-HRMS calcd. for $C_{39}H_{39}N_4O_7Ru_2$ [Ru_2(bbpmp)$(OAc)_2^+$] 879.0900: found 879.0902. $C_{43}H_{51}N_5O_{12}Ru_2$ [Ru_2(bbpmp)$(OAc)_3 \cdot CH_3CN \cdot 3H_2O$] (1032.04): calcd. C 50.04, H 4.98, N 6.79; found C 49.95, H 4.85, N 6.60. Single crystals suitable for X-ray crystallography were obtained by vapour diffusion of toluene into an acetonitrile solution of **4**.

Synthesis of Co_2(bbpmp)(OAc)(OMe)(PF_6) (5): Ligand **3** (0.50 g, 0.89 mmol) was suspended in MeOH (15 mL). $Co(OAc)_2{\cdot}4H_2O$ (0.46 g, 1.8 mmol) was added, and the colour turned brown. After addition of NaOAc (0.22 g, 2.7 mmol), the reaction mixture was heated at reflux overnight and then centrifuged. A pink insoluble solid was separated from the brown solution. To this brown solution was added a saturated aqueous solution of KPF_6 (5 mL), and the solution was put in a refrigerator. After a couple of days a brown precipitate had formed, which was filtered, washed with H_2O and Et_2O and then dried (0.35 g, 43%). IR (KBr disc): $\tilde{\nu}$ = 3413 (br.), 2918, 2842, 1560, 1477, 1412, 1266, 1017, 758 cm^{-1}. ESI-HRMS calcd. for $C_{38}H_{39}Co_2N_4O_6$ [Co_2(bbpmp)(OAc)(OMe)$^+$] 765.1528; found 765.1523. $C_{42}H_{49}Co_2F_6N_4O_7P$ [Co_2(bbpmp)-(OAc)(OMe)(PF_6)·Et_2O] (984.70): calcd. C 51.23, H 5.02, N 5.69; found C 52.70, H 5.00, N 5.60. Single crystals suitable for X-ray crystallography were obtained by vapour diffusion of toluene into an acetonitrile solution of **5**.

Synthesis of Cu_4(Hbbpmp)$_2$(OAc)$_2$(H_2O)$_2$(PF_6)$_2$ (6): Ligand **3** (0.45 g, 0.80 mmol) was suspended in MeOH (15 mL). When $Cu(OAc)_2{\cdot}4H_2O$ (0.46 g, 1.8 mmol) was added, the colour turned green. After heating at reflux overnight, a saturated aqueous solution of KPF_6 (12 mL) was added, and a green precipitate was formed. The mixture was put in the refrigerator overnight for full precipitation. The solution was centrifuged, and the green solid was washed with H_2O followed with Et_2O, and finally dried (0.64 g, 90%). IR (KBr disc): $\tilde{\nu}$ = 3600, 3400 (br.), 2908, 2950, 1611, 1565, 1476, 1446, 1380, 1268, 1112, 1083, 1029, 841, 758 cm^{-1}. ESI-HRMS calcd. for $C_{35}H_{33}Cu_2N_4O_3$ [Cu_2(bbpmp)$^+$] 683.1139; found 683.1140. $C_{74}H_{86}Cu_4F_{12}N_8O_{16}P_2$ [Cu_4(Hbbpmp)$_2$(OAc)$_2$(H_2O)$_2$-(PF_6)$_2$·$4H_2O$] (1887.64): calcd. C 47.09, H 4.59, N 5.94; found C 46.20, H 4.10, N 5.95. Plate-shaped crystals suitable for X-ray crystallography were obtained by vapour diffusion of toluene into an acetonitrile solution of **6**.

General Procedure for the Catalytic Oxidations of Alcohols with the Ru dimer 4: To a solution of the catalyst (3.0 mg, 0.003 mmol) and dodecane (33.3 μL, 0.15 mmol) in a mixture of freshly distilled thf and acetonitrile (1:1, 1.0 mL) was added the substrate (0.15 mmol) followed by the oxidant iodobenzene diacetate (0.193 g, 0.60 mmol). Finally, the mixture was flushed with argon and stirred at 40 °C. Aliquots were taken and filtered through a silica plug and analyzed by GC.

General Procedure for the Biomimetic Acetoxylation with the Co dimer 5: $Pd(OAc)_2$ (7.6 mg, 0.034 mmol), the Co dimer **5** (12.5 mg, 0.014 mmol), hydroquinone (15.0 mg, 0.14 mmol) and $LiOAc{\cdot}2H_2O$ (22.5 mg, 0.14 mmol) were dissolved in AcOH (2 mL) and stirred in air for 20 min. The reaction flask was sealed, degassed and purged with oxygen, and finally, the substrate (0.68 mmol) was added. After stirring at 50 °C for 6–24 h, the reaction mixture was diluted with water and extracted with pentane or dcm. The organic phases were combined, washed with water, saturated aqueous solution of $NaHCO_3$ and dried with $MgSO_4$. The solution was filtered and carefully evaporated to yield the product.

Aerobic Oxidation of 3,5-Di-*tert*-butylcatechol with Complex 6: Stock solutions of catalyst **6** (0.5 mM) and 3,5-di-*tert*-butylcatechol (0.18 M) in MeOH were prepared. A cuvette with a stirring bar was charged with MeOH (2.56 mL) saturated with O_2, followed by aqueous tris buffer pH 8.0 (200 μL, 2.7 M) and a solution of 3,5-di-*tert*-butylcatechol (100 μL) ([3,5-dtbc]$_0$ ≈ 6.0 mM). Finally, the reaction was initiated by the addition of a solution of complex **6** (144 μL, [**6**]$_0$ ≈ 24 μM) at ambient temperature. Oxidation was observed spectrophotometrically by an increase in the characteristic absorption band of the product 3,5-di-*tert*-butyl-*o*-benzoquinone at 406 nm.

Supporting Information (see footnote on the first page of this article): X-ray structures and selected bond lengths and angles of **4**, **5**, and **6** are presented.

Acknowledgments

We thank Dr. Junliang Sun and Professors Licheng Sun and Jan-E. Bäckvall for discussions and The Knut & Alice Wallenberg Foundation, The Swedish Research Council, and The Göran Gustafsson Foundation for financial support.

[1] a) W. Rüttinger, G. C. Dismukes, *Chem. Rev.* **1997**, *97*, 1–24; b) L. Sun, L. Hammarström, B. Åkermark, S. Styring, *Chem. Soc. Rev.* **2001**, *30*, 36–49; c) M. Yagi, M. Kaneko, *Chem. Rev.* **2001**, *101*, 21–36; d) B. Loll, J. Kern, W. Saenger, A. Zouni, J. Biesiadka, *Nature* **2005**, *438*, 1040–1044; e) K. N. Ferreira, T. M. Iverson, K. Maghlaoui, J. Barber, S. Iwata, *Science* **2004**, *303*, 1831–1838.

[2] a) J. Limburg, J. S. Vrettos, H. Y. Chen, J. C. de Paula, R. H. Crabtree, G. W. Brudvig, *J. Am. Chem. Soc.* **2001**, *123*, 423–430; b) J. Limburg, G. W. Brudvig, R. H. Crabtree, *J. Am. Chem. Soc.* **1997**, *119*, 2761–2762; c) W. Rüttinger, M. Yagi, K. Wolf, S. Bernasek, G. C. Dismukes, *J. Am. Chem. Soc.* **2000**, *122*, 10353–10357; d) A. K. Poulsen, A. Rompel, C. J. McKenzie, *Angew. Chem. Int. Ed.* **2005**, *44*, 6916–6920; e) Y. Naruta, M.-A. Sasayama, T. Sasaki, *Angew. Chem. Int. Ed. Engl.* **1994**, *33*, 1839–1841; f) Y. Gao, J. Liu, M. Wang, Y. Na, B. Åkermark, L. Sun, *Tetrahedron* **2007**, *63*, 1987–1994; g) Y. Gao, T. Åkermark, J. Liu, L. Sun, B. Åkermark, *J. Am. Chem. Soc.* **2009**, *131*, 8726–8727; h) C. W. Cady, R. H. Crabtree, G. W. Brudvig, *Coord. Chem. Rev.* **2008**, *252*, 444–455; i) G. Berggren, Dissertation, Uppsala University, **2009**, pp. 22–28; j) S. Mukhopadhyay, S. K. Mandal, S. Bhaduri, W. H. Armstrong, *Chem. Rev.* **2004**, *104*, 3981–4026.

[3] a) J. A. Gilbert, D. S. Eggleston, W. R. Murphy, D. A. Geselowitz, S. W. Gersten, D. G. Hodgson, T. J. Meyer, *J. Am. Chem. Soc.* **1985**, *107*, 3855–3864; b) S. W. Gersten, G. J. Samuels, T. J. Meyer, *J. Am. Chem. Soc.* **1982**, *104*, 4029–4030; c) T. J. Meyer, *Acc. Chem. Res.* **1989**, *22*, 163–170.

[4] a) F. Liu, J. J. Concepción, J. W. Jurss, T. Cardolaccia, J. L. Tempelton, T. J. Meyer, *Inorg. Chem.* **2008**, *47*, 1727–1752; b) X. Sala, I. Romero, L. Escriche, A. Llobet, *Angew. Chem. Int. Ed.* **2009**, *48*, 2842–2852; c) Z. Deng, H.-W. Tseng, R. Zong, D. Wang, R. Thummel, *Inorg. Chem.* **2008**, *47*, 1835–1848; d) Y. Xu, T. Åkermark, V. Gyollai, D. Zou, L. Eriksson, L. Duan, R. Zhang, B. Åkermark, L. Sun, *Inorg. Chem.* **2009**, *48*, 2717–2719; e) L. Duan, A. Fischer, Y. Xu, L. Sun, *J. Am. Chem. Soc.* **2009**, *131*, 10397–10399.

[5] M. F. Anderlund, J. Zheng, M. Ghiladi, M. Kritikos, E. Rivière, L. Sun, J.-J. Girerd, B. Åkermark, *Inorg. Chem. Commun.* **2006**, *9*, 1195–1198.

[6] B. Krebs, K. Schepers, B. Bremer, G. Henkel, E. Althaus, W. Müller-Warmuth, K. Griesar, W. Haase, *Inorg. Chem.* **1994**, *33*, 1907–1914.

[7] A. Neves, M. A. de Brito, I. Vencato, V. Drago, K. Griesar, W. Haase, *Inorg. Chem.* **1996**, *35*, 2360–2368.

[8] N. L. Fry, M. J. Rose, D. L. Rogow, C. Nyitray, M. Kaur, P. K. Mascharak, *Inorg. Chem.* **2010**, *49*, 1487–1495.

[9] L. Gong, S. P. Mulcahy, K. Harms, E. Meggers, *J. Am. Chem. Soc.* **2009**, *131*, 9602–9603.

[10] C.-F. Leung, S. M. Ng, J. Xiang, W.-Y. Wong, M. H.-W. Lam, C.-C. Ko, T.-C. Lau, *Organometallics* **2009**, *28*, 5709–5714.

[11] Z.-J. Xu, R. Fang, C. Zhao, J.-S. Huang, G.-Y. Li, N. Zhu, C.-M. Che, *J. Am. Chem. Soc.* **2009**, *131*, 4405–4417.

[12] M. Gatti, L. Vielle-Petit, X. Luan, R. Maritz, E. Dinkel, A. Linden, R. Dorta, *J. Am. Chem. Soc.* **2009**, *131*, 9498–9499.

[13] A. R. Paital, M. Sarkar, M. Mikuiya, D. Ray, *Eur. J. Inorg. Chem.* **2007**, 4762–4769.
[14] A. Neves, L. R. Rossi, I. Venkato, V. Drago, W. Haase, R. Werner, *Inorg. Chim. Acta* **1998**, *281*, 111–115.
[15] A. Neves, L. M. Rossi, A. J. Bortoluzzi, B. Szpoganicz, C. Wiezbicki, E. Schwingel, S. Ostrovsky, W. Haase, *Inorg. Chem.* **2002**, *41*, 1788–1794.
[16] R. Lomoth, A. Magnuson, Y. Xu, L. Sun, *J. Phys. Chem. A* **2003**, *107*, 4373–4380.
[17] T. Norrby, A. Börje, B. Åkermark, L. Hammarström, J. Alsins, K. Lashgari, R. Norrestam, J. Mårtensson, G. Stenhagen, *Inorg. Chem.* **1997**, *36*, 5850–5858.
[18] Y. Xu, unpublished results.
[19] a) For a recent overview, see: W. C. Arends, R. A. Sheldon in *Modern Oxidation Methods* (Ed.: J.-E. Bäckvall), Wiley VCH Verlag, Weinheim, **2004**, p. 83–118; b) F. H. Jardine, *Prog. Inorg. Chem.* **1984**, *31*, 265–370; c) C. Bilgrien, S. Davis, R. S. Drago, *J. Am. Chem. Soc.* **1987**, *109*, 3786–3787.
[20] J. Piera, J.-E. Bäckvall, *Angew. Chem. Int. Ed.* **2008**, *47*, 3506–3523.
[21] a) S. E. Byström, E. M. Larsson, B. Åkermark, *J. Org. Chem.* **1990**, *55*, 5674–5675; b) J.-E. Bäckvall, R. B. Hopkins, H. Grennberg, M. Mader, A. K. Awasthi, *J. Am. Chem. Soc.* **1990**, *112*, 5160.
[22] a) J.-E. Bäckvall, R. L. Chowdhury, U. Karlsson, *J. Chem. Soc., Chem. Commun.* **1991**, 473; b) G.-Z. Wang, U. Andreasson, J.-E. Bäckvall, *J. Chem. Soc., Chem. Commun.* **1994**, 1037; c) G. Csjernyik, A. H. Éll, L. Fadini, B. Pugin, J.-E. Bäckvall, *J. Org. Chem.* **2002**, *67*, 1657–1662.
[23] J.-E. Bäckvall, R. B. Hopkins, *Tetrahedron Lett.* **1988**, *29*, 2885–2888.
[24] G. M. Sheldrick, *Acta Crystallogr., Sect. A* **2008**, *64*, 112–122.
[25] A. L. Spek, *J. Appl. Crystallogr.* **2003**, *36*, 7–13.
[26] C. Hormillosa, *VALENCE*, Version 2.00, Institute for Materials Research, McMaster University, **1993**.

Received: July 12, 2010
Published Online: October 22, 2010

